

Spectroscopic studies of vanadium incorporated SAPO-11

Puyam S. Singh, Rajib Bandyopadhyay, B.S. Rao *

Catalysis Division, National Chemical Laboratory, Pune, 411 008, India

Received 3 March 1995; accepted 22 May 1995

Abstract

The incorporation of vanadium during the hydrothermal synthesis of SAPO-11 is reported. The sample is characterized by different spectroscopic techniques namely XRD, ESR, TPR, UV–VIS and ^{51}V MAS-NMR. ESR, UV–VIS and ^{51}V MAS-NMR studies reveal that vanadium in VAPSO-11 is located in square pyramidal or distorted octahedral structures. Vanadium shows redox behaviour (V^{4+} to V^{5+} and vice versa) when calcined and reduced. Samples prepared by impregnation of vanadium into SAPO-11 (V-SAPO-11) are compared with VAPSO-11.

Keywords: Vanadium; SAPO-11; VAPSO-11; ESR; TPR; ^{51}V MAS-NMR

1. Introduction

Microporous crystalline aluminophosphates belong to a class of solids with potential use as adsorbents and catalysts [1]. Substitution of phosphorous by silicon in the ALPO- n gives SAPO- n , n being the particular structure type. Incorporation of metal ion in ALPO- n and SAPO- n gives MeAPO- n and MeAPSO- n (Me denotes metal), respectively.

The incorporation of vanadium in silicalite [2,3] and ALPO- n [4] has been reported. However, successful incorporation of vanadium into the framework is still controversial. The incorporation of vanadium in ALPO and SAPO is interesting in catalytic reactions as these incorporation exhibit oxidative and acidic properties. Montes et al. [5] have reported that in VAPO-5, V^{4+} , V^{5+} substitute P^{5+} within the aluminophosphate framework. More recently, Rigutto et al. [6] have

reported that vanadium in VAPO-5 occupies aluminium rather than phosphorous sites. In the present paper we report the synthesis and spectroscopic studies of vanadium incorporation in ALPO-11 and SAPO-11.

2. Experimental

2.1. Synthesis

ALPO-11 and SAPO-11 were synthesized hydrothermally according to known procedures [7]. An aluminophosphate gel was prepared by mixing aluminium isopropoxide (Aldrich) with 85% orthophosphoric acid (Merck) and deionized water. An organic additive (n-dipropyl amine, Aldrich) was added and the final gel was stirred for 10–15 min. For SAPO-11 synthesis, silica sol (Ludox AS-40) was added to the aluminophosphate gel before the addition of the organic addi-

* Corresponding author. Fax: (+91-212)334761.

tive. An aqueous solution containing appropriate amount of V^{4+} was prepared by dissolving $VOSO_4 \cdot 5H_2O$ in deionized water. This was added to the aluminophosphate and silicoaluminophosphate gel before the addition of the organic additive in the synthesis of vanadium incorporated ALPO-11 and SAPO-11, designated as VAPO-11 and VAPSO-11 respectively. Molar composition of the reaction mixture for the synthesis of ALPO-11, SAPO-11, VAPO-11 and VAPSO-11 are given in Table 1. The gel was then transferred into an autoclave and heated at 473 K for 24 h. The crystallized material was filtered and washed thoroughly with deionized water. The samples were calcined at 823 K for 24 h in air to remove the organic additive.

Vanadium was impregnated on ALPO-11 and SAPO-11 according to the following procedure. One gram of calcined sample was added to 100 ml of $VOSO_4 \cdot 5H_2O$ (0.26 wt.%, in water) solution and stirred at 363 K until complete dryness. The sample was then washed thoroughly with deionized water to remove surface vanadium. These samples are denoted as V-ALPO-11 and V-SAPO-11.

2.2. Characterization

The synthesized samples were characterized by XRD (Rigaku, Model D/MAX-VC, with $CuK\alpha$

radiation, Ni filter, $\lambda = 1.5404 \text{ \AA}$). Thermal analysis of the samples was performed on a derivatograph (Setaram TG-DTA 92) at a rate of $10^\circ\text{C}/\text{min}$ using α -alumina as a reference material. X-band ESR spectra were recorded at 300 K and 77 K (Bruker-E 2000) with a rectangular cavity ST_{9424} using a standard sample, weak pitch variation, $g = 2.0029$. ^{51}V MAS-NMR spectra were obtained at room temperature (Bruker MSL-300, operating in Fourier transform mode using 'one cycle' type measurement). The sorption measurements were carried out on an all glass gravimetric apparatus using a McBain–Baker type silica spring (sensitivity = 70 cm/g). Temperature programmed reduction (TPR) spectra for V_2O_5 and vanadium containing molecular sieve were recorded using an automated instrument (Sorbs-tar, Model 200) with a thermal conductivity detector, the carrier gas being 5% H_2 in argon, v/v.

3. Results and discussion

Table 1 reveals molar composition of the reaction mixture for the synthesis of ALPO-11 and related structures; the molar chemical composition and unit cell composition of final crystalline samples. In SAPO-11, nearly half the amount of input concentration of silica is incorporated. The

Table 1
Molar composition of the reaction mixture for the synthesis of ALPO-11 and related structures and unit cell composition of crystalline samples

Synthesis batch composition ^a							Unit cell composition of crystallized sample (on anhydrous basis)
Sample	Al_2O_3 :	P_2O_5 :	SiO_2 :	V_2O_5 :	H_2O :	DPA	
ALPO-11	1 (1)	1 (1)	0	0	40	1	$Al_{20}P_{20}O_{80}$
SAPO-11	1 (0.90)	1 (0.80)	0.6 (0.30)	0	40	1	$H_{3.16}Si_{3.16}Al_{19.28}P_{17.05}O_{80}$
VAPO-11	0.93 (0.94)	1 (1.03)	0	0.070 (0.028)	40	1	$V_{0.56}Al_{20.57}P_{18.82}O_{80}$
VAPSO-11 (L)	0.98 (0.91)	1 (0.80)	0.6 (0.29)	0.011 (0.006)	40	1	$H_{3.10}V_{0.13}Si_{3.10}Al_{19.64}P_{17.15}O_{80}$
VAPSO-11 (H)	0.93 (0.90)	1 (0.79)	0.6 (0.29)	0.067 (0.030)	40	1	$H_{3.08}V_{0.61}Si_{3.08}Al_{19.33}P_{16.98}O_{80}$

^a The figures in parentheses indicate the final molar composition of the crystallized samples.

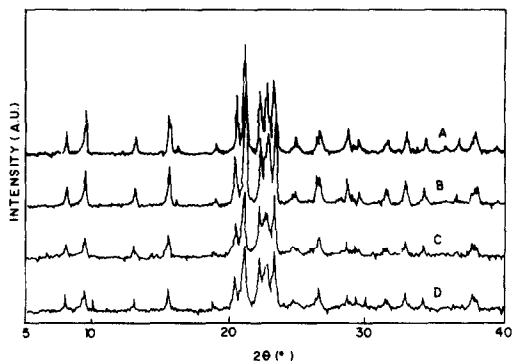


Fig. 1. XRD patterns of synthesized samples (A) ALPO-11, (B) SAPO-11, (C) VAPO-11 and (D) VAPSO-11.

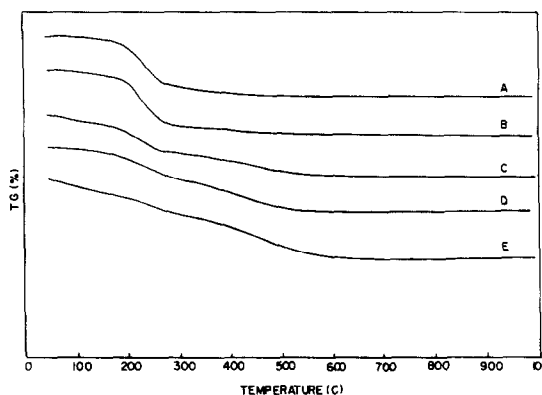


Fig. 2. TG patterns of synthesized samples (A) ALPO-11, (B) VAPO-11 (C) SAPO-11, (D) VAPSO-11 (0.584% V) and (E) VAPSO-11 (2.64% V).

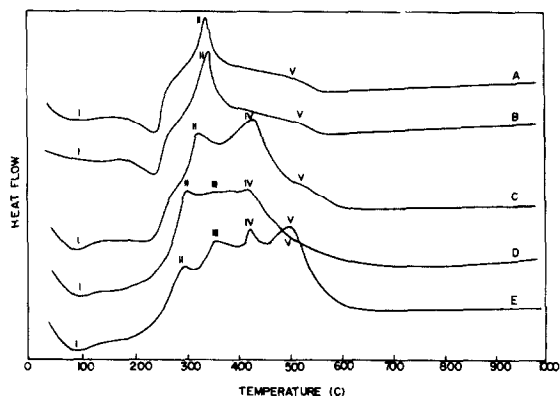


Fig. 3. DTA patterns of synthesized samples (A) ALPO-11, (B) VAPO-11 (C) SAPO-11, (D) VAPSO-11 (0.584% V) and (E) VAPSO-11 (2.64% V).

percentage of silicon incorporation of the total input concentration of silica is nearly the same in all silicon containing samples. For VAPO-11 and VAPSO-11, nearly 40–50% of the total amount of vanadium is incorporated. XRD powder pat-

terns (Fig. 1) of VAPSO-11 are similar to ALPO-11, SAPO-11 and VAPO-11 indicating the presence of an AEL type framework structure. On calcination the colour of the VAPSO-11 samples turned from greenish white to yellow due to the oxidation of V^{4+} to V^{5+} without any change in the XRD pattern. Thermal analysis of ALPO-11, SAPO-11, VAPO-11 and VAPSO-11 with two different vanadium content are shown in Fig. 2 and Fig. 3. The thermoanalytical curves of SAPO-11 and VAPSO-11 reveal that calcination process under air proceeds in five stages, as in case of MeAPSO-11 (Me = Mg, Zn, Mn, Cd, Ni or Cr) [8]. Stage I shows endothermic desorption of water. Stages II–V reveal the oxidative decomposition of the template molecules and in all these stages, exothermic peaks are observed. For ALPO-11, the main process of the removal of template proceeds under stage II which is in accordance with the reported literature [9]. A certain amount of template acts as charge compensating anion which interacts with the weak acid centres of ALPO-11. It can be noted that ALPO-11 possesses weak acid centres [10], originated from terminal hydroxyl bands (T-OH, T = Al or P) and lattice defect sites induced Lewis acid sites. VAPO-11 shows similar thermoanalytical curve as compared to ALPO-11. For SAPO-11, the removal of the template under stage III is extremely weak. The main process of the decomposition of the template proceeds in stages II and IV. Certain amounts of template are converted into coke during the calcination and strongly interact with cationic framework, which can be burned out in air during stage V at higher temperature. A replacement of Al^{3+} by $[VO]^{3+}$ in the lattice does not create any additional framework charge. However, broadening in the exothermic peak under stages II to V is observed. VAPSO-11(L) with low vanadium content (0.584%), compared to SAPO-11 shows slightly pronounced DTA peaks under stages III and V. VAPSO-11(H) with high vanadium content (2.64% V) shows more pronounced peaks in all stages of template decomposition. The diffusibility of template during calcination of sample depends upon the state of

Table 2
Sorption capacity (wt.%) at 298 K and $p/p_0=0.8$

Adsorbate	ALPO-11	SAPO-11	VAPO-11	VAPSO-11
Cyclohexane	5.1	4.9	4.1	3.5
H ₂ O	17.0	17.2	8.0	9.0

template, anchored inside the pore. The template is in occluded form in the pores of ALPO-11. Such occluded template is removed freely under stage II during calcination. However, some template molecules interact strongly with the stronger acid sites of the sample and are not able to diffuse freely. Such phenomena are seen in acidic SAPO-11 and more clearly in vanadium containing SAPO-11. Sorption capacities of water and cyclohexane are given in Table 2. The sorption capacity of VAPSO-11 is nearly similar to that of VAPO-11 reported earlier [4]. The sorption capacities of cyclohexane and water are 15% lower and 13% higher respectively for VAPSO-11 than VAPO-11. However, compared to ALPO-11, SAPO-11; the sorption capacities of both cyclohexane and water decrease for vanadium containing ALPO and SAPO molecular sieve. The introduction of vanadium in the synthesis decreases the porosity of the sample. The exact correlation between vanadium content and decrease in porosity could not be concluded. An attempt was made to exchange extra-framework vanadium [11] by treating 2 g of VAPSO-11 with 100 ml 5% ammonium acetate solution. No vanadium is detected in the leached out solution.

The esr spectra of V^{4+} in VAPO-11, VAPSO-11 (as-synthesized, calcined, reduced) recorded at 298 K and 77 K (Fig. 4) show the presence of V^{4+} in a distorted octahedral environment. ESR spectra of tetrahedrally coordinated $3d^1$ transition metals can only be observed at low temperatures. On the other hand, octahedrally coordinated $3d^1$ transition metals can easily be seen even at room temperature. There is no increase of intensity in the spectrum of V^{4+} at 77 K. However, the absence of V^{4+} in tetrahedrally coordinated environment can not be concluded by the similarity between spectra at 298 K and 77 K. Some EPR

invisible V^{4+} could be present even at the liquid N_2 temperature. The intensity in the spectrum decreases sharply with the increase in calcination temperature indicating the oxidation of V^{4+} to V^{5+} . The anisotropic hyperfine splitting caused by the ^{51}V nucleus is well resolved in all the samples indicating good dispersion and immobility of the vanadium species.

Table 3 gives the ESR parameters for some vanadyl complexes and vanadium incorporated molecular sieves [12–16]. Vanadyl complexes usually show C_{4v} symmetry, coordinated to other groups both in the solid state and in solution. Under C_{4v} symmetry the energy levels of d electrons are split up. The splitting of $\Delta E(^2B_2 - ^2B_1)$ (or $b_2(xy) \rightarrow b_1(x_2 - y_2)$) does not depend on tetragonal distortion whereas $\Delta E(^2B_2 - ^2E_1)$ (or $b_2(xy) \rightarrow e\pi^x(xz, yz)$) is a measure of this distortion. Kivelson and Lee [17] determined the

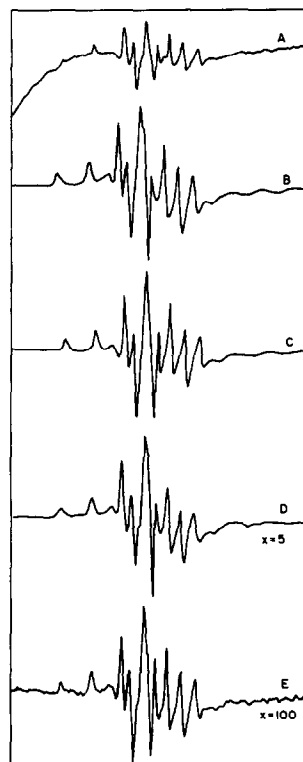


Fig. 4. ESR spectra of samples (A) VAPO-11 (synthesized), (B) VAPSO-11 (synthesized), (C) VAPSO-11 (calcined and reduced), (D) VAPSO-11 (calcined at 573 K) and (E) VAPSO-11 (calcined at 773 K) ($x=5$ and $x=100$ denote magnifications by 5 and 100, respectively).

Table 3

ESR parameters g_{\parallel} , g_{\perp} , A_{\parallel} , A_{\perp} measured by ESR for some vanadyl complexes and vanadium incorporated silicalite, aluminosilicate, aluminophosphate

Complex/sample	Geometry	β_2^{*2}	g_{\parallel}	g_{\perp}	A_{\parallel}^a	A_{\perp}^a	$\Delta g_{\parallel}/\Delta g_{\perp}$	Ref.
VOSO ₄ ·5H ₂ O	Oh ^b		1.99					[9]
VAPO-11(S) ^c	Oh	0.980	1.925	1.993	184	67	8.312	PW ^h
VAPSO-11(S) ^c	Oh	1.015	1.924	1.993	188	67	8.419	PW
VAPSO-11(573) ^f	Oh	1.009	1.925	1.994	187	67	9.31	PW
VAPSO-11(773) ^f	Oh	1.001	1.928	1.994	186	67	8.95	PW
VAPSO-11(R) ^g	Oh	1.000	1.927	1.994	188	69	9.07	PW
V-ZSM-5	Oh	0.908	1.925	1.975	181.5	75.5	2.831	[13]
V-Silicalite(S) ^c	Oh	0.947	1.935	1.994	183	69	8.108	[3]
V-Silicalite	Oh	0.945	1.932	1.976	182	69.5	2.673	[13]
VAPO-5(S) ^{c,r}	Oh	0.996	1.931	1.991	188	70.1	6.309	[6]
	Oh	0.997	1.934	1.993	189.8	72	7.344	[6]
VAPO-5(S) ^{c,m}	Oh	0.947	1.932	1.983	185	73	3.642	[5]
	Oh	0.945	1.935	1.983	180	68.2	3.487	[5]
(VO, Mg)(NH ₄) ₂ (SO ₄) ₂ ·6H ₂ O	Oh	0.887	1.914	1.979	180	73	3.790	[10]
(VO, Cd)SO ₄ ·8/3H ₂ O	Oh	0.927	1.912	1.975	188	76	3.308	[10]
(VO, K)SO ₄ ·7H ₂ O	Oh	0.916	1.925	1.973	177	68	2.638	[10]
Cs(Al, VO)(SO ₄) ₂ ·12H ₂ O	Oh	0.994	1.932	1.979	183	66	3.017	[11]
VO(salen) ^d	Sq.Py. ^c	0.938	1.949	1.985	165.9	57	3.081	[12]

^a A_{\parallel} and A_{\perp} in units 10^{-4} cm^{-1} .^b Octahedral.^c Square pyramidal.^d Salen: bis(salicylaldehyde)ethylenediimine.^e Hydrothermal synthesis.^f Figures in parentheses are calcination temperatures in K.^g Calcined and reduced.^h PW = present work.^r Ref. [6].^m Ref. [5].

appropriate values of g factors using the following equations.

$$\Delta g_{\parallel} = g_{\parallel} - g_e = - (8\lambda\beta_1^{*2}\beta_2^{*2}) / \Delta E(2B_2 - 2B_1) \quad (1)$$

$$\Delta g_{\perp} = g_{\perp} - g_e = - (2\lambda\beta_2^{*2}e\pi^{*2}) / \Delta E(2B_2 - 2E_1) \quad (2)$$

where λ is the spin orbit coupling constant for a free ion, and β_2^{*2} describes the degree of delocalization of an unpaired electron.

From Eqs. 1 and 2

$$\Delta g_{\parallel} / \Delta g_{\perp} = 4\beta_1^{*2} \Delta E(2B_2 - 2E_1) / e\pi^{*2} \Delta E(2B_2 - 2B_1) \quad (3)$$

The distance of vanadium and oxygen in VO²⁺ group directly relates with $\Delta g_{\parallel} / \Delta g_{\perp}$ ratio and

hyperfine interaction constant A_{\parallel} . When the $\Delta g_{\parallel} / \Delta g_{\perp}$ ratio or A_{\parallel} is increased there is a decrease V=O bond and shortening in the lengths of the bonds between the vanadium ion and the equatorial ligands [18–21]. $\Delta g_{\parallel} / \Delta g_{\perp}$ ratio is higher for VAPSO-11 than other vanadium containing aluminophosphate molecular sieves indicating V=O bond distance is shorter. The nature and location of vanadium in hydrothermally synthesized vanadium silicalite is different from other types of preparation. In the method used by Whittington et al., the calcined sample (silicalite or ZSM-5) is treated with VOCl₃ for 1 h. $\Delta g_{\parallel} / \Delta g_{\perp}$ for vanadium silicalite and V-ZSM-5, prepared by this solid state exchange method is 2.673 and 2.831 respectively, whereas $\Delta g_{\parallel} / \Delta g_{\perp}$ for hydrothermally synthesized vanadium silicalite is 8.108.

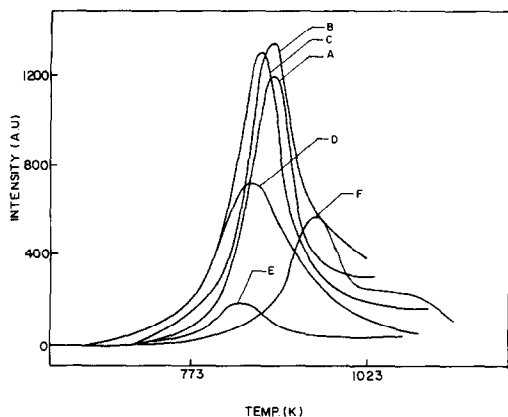


Fig. 5. TPR spectra of samples (A) V-SAPO-11, (B) V-ALPO-11, (C) VAPO-11, (D) VAPSO-11, (E) VS-1 and (F) 4% (wt.%) V_2O_5 in SAPO-11 matrix.

Similarly, $\Delta g_{\parallel} \Delta g_{\perp}$ for hydrothermally synthesized VAPO-11 and VAPSO-11 is 8.312 and 8.419 respectively. The $\Delta g_{\parallel} / \Delta g_{\perp}$ remain nearly constant for calcined VAPSO-11 sample and its reduced form after calcination. For hydrothermally synthesized VAPO-5 by Rigutto et al., [6] $\Delta g_{\parallel} / \Delta g_{\perp}$ is 6.309 and 7.344. However, $\Delta g_{\parallel} / \Delta g_{\perp}$ for VAPO-5 synthesized by Montes et al., is 3.642 and 3.487. The change in $\Delta g_{\parallel} / \Delta g_{\perp}$ value clearly reveals that the incorporation of vanadium in the framework of ALPO molecular sieve is dependent on the method of incorporation and on crystal structure of the porous solid material like V-Silicalite, VAPO-11 or VAPO-5. It can be noted from the studies by Brouet et al. [22] that MnAPO-5 contains mostly extra-framework manganese whereas MnAPO-11 contains mostly framework manganese.

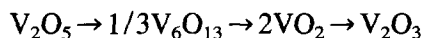
The delocalization coefficient (β_2^{*2}) of the π -

bond in V=O can be calculated using the following equation given by Kivelson and Lee [17]. For β_2^{*2} approaching unity the π bond to the ligands in the xy plane is highly ionic.

$$\beta_2^{*2} = 7/6[\Delta g_{\parallel} - 5/14\Delta g_{\perp} - (A_{\parallel} - A_{\perp})/P]$$

The value of P is assumed to be $128 \times 10^{-4} \text{ cm}^{-1}$ by many researchers [20,23] and found to be correct. For V^{4+} in hydrothermally synthesized vanadium containing molecular sieve, β_2^{*2} value is nearly 1 which shows that π bond of V=O is highly ionic.

Fig. 5 and Table 4 give the results of TPR of different vanadium containing samples along with the physical mixture of V_2O_5 and SAPO-11. It has been reported [24] that the reduction of V_2O_5 by TPR spectra proceeds as follows



However, Roozeboom et al. [25] found one single reduction at ca. 800 K for V_2O_5 . The step for the formation of monoclinic V_6O_{13} is not resolved in our study.

Since the maximum temperature of reduction (V^{5+} to V^{4+}) is related to the strength of the V–O–M (M = Si or Al or P) and not on the coordination of vanadium, the reducibility of vanadium can be explained. The increase of maximum temperature of reduction of vanadium in VS-1 < VAPSO-11 < VAPO-11 is probably due to stronger V–O–P bond. Further shifting of maximum temperature of reduction in V-ALPO-11 and V-SAPO-11 characterized a relatively stronger metal interaction between less dispersed vana-

Table 4
TPR results of vanadium containing molecular sieves^a

Catalyst	Temp. of peak maximum (K)	Vanadium content wt.% (g/100 g)	
		Area %	Chemical analysis
VAPSO-11	856	2.53	2.64
VAPO-11	869	2.44	2.45
V-SAPO-11	883	4.55	5.00
V-ALPO-11	886	4.50	4.89
VS-1	843	0.90	1.00
4% (wt.%) V_2O_5 in SAPO-11	944, 1053	2.12	2.15

^a Conditions: carrier gas: 5% H_2 in argon; heating rate: 16 K/min; flow: 25 ml/min; sample wt.: 300 mg.

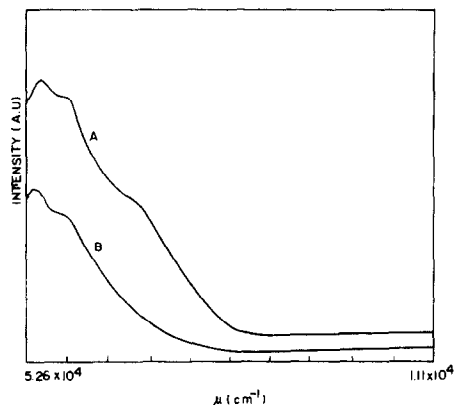


Fig. 6. UV-VIS spectra of samples (A) VAPSO-11 and (B) V-SAPO-11.

dium species. This is further confirmed by characterizing physically mixed 4% V_2O_5 in SAPO-11. For physically mixed 4% V_2O_5 in SAPO-11, the relative maximum temperature of reduction (V^{5+} to V^{4+}) is observed at 944 K and a smaller line at higher temperature (1053 K) indicates reduction of V^{4+} to V^{3+} . The reduction of V^{4+} to V^{3+} could not be observed in vanadium-incorporated or impregnated AEL type structure.

Calcined VAPSO-11 reveals two main absorption bands at around $37,594\text{ cm}^{-1}$, $45,662\text{ cm}^{-1}$ and a shoulder at $26,042\text{ cm}^{-1}$. The shoulder at $26,042\text{ cm}^{-1}$ was not seen in V-SAPO-11 (Fig. 6). Centi et al. [11] assigned the band at around $26,042$, $37,594$ and $45,662\text{ cm}^{-1}$ to the presence of a $V=O$ bond and near-square pyramidal field respectively. The attribution of V^{5+} species characterized by UV-Visible spectra suggests a short $V=O$ bond and three slightly longer $V-O$ bonds and a loosely bonded $V-O-P$ indicating square pyramidal vanadyl species.

Fig. 7 shows the ^{51}V MAS-NMR spectra of as-synthesized and calcined VAPSO-11 samples. Rigutto et al. [6] studied possible environments for V^{5+} sites in VAPO-5 materials using vanadyl(V) phosphate ($VOPO_4$) and aluminium orthovanadate ($AlVO_4$) as the model compounds. For β - $VOPO_4$, the static spectrum shows features indicative of a large quadrupolar coupling constant. The isotropic shift was found to be $-757 \pm 2\text{ ppm}$ by means of magic angle spinning at different speeds (3–7.5 kHz). This can arise

from vanadium in an environment having a square pyramidal or distorted octahedral coordination. This geometry of β - $VOPO_4$ is characterized by a chemical shift tensor of approximate axial symmetry which dominates the spectrum, with σ_{\perp} being usually between -200 and -400 ppm and σ_{\parallel} between -800 and -1300 ppm [26]. For tetrahedral vanadium(V) as in orthovanadates the anisotropy is relatively small and the signals are centered around -500 to -600 ppm [26,27]. The static ^{51}V NMR spectra of calcined VAPSO-11 shows a broad signal with upfield at 300 ppm and extends upto 900 ppm . ^{51}V MAS-NMR spectra of the calcined VAPSO-11 sample (Fig. 7 B) shows narrow chemical shift distribution with the central band of -540 ppm . The ^{51}V MAS-NMR pattern is consistent with previously published literature of predicted square pyramidal or distorted octahedral vanadyl(V) species in VAPO-5 [6]. For VAPO-11, similar absorption pattern of ^{51}V MAS-NMR spectra is observed.

The oxidation state of vanadium which remains intact in the as-synthesized VAPSO-11 framework is mostly V^{4+} state as described above. A small fraction of V^{5+} may possibly be located in the extra-framework position of VAPSO-11. ^{51}V

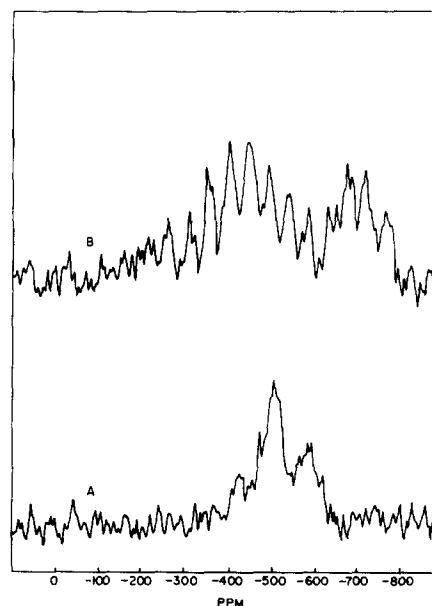


Fig. 7. ^{51}V MAS NMR spectra of samples (A) VAPSO-11 (as-synthesized) and (B) VAPSO-11 (calcined).

MAS-NMR spectrum of as-synthesized VAPSO-11 (Fig. 7 A) shows the presence of a tetrahedral V^{5+} species with a central band signal around -500 ppm. Thus the presence of a small amount of tetrahedral V^{5+} cannot be excluded in calcined VAPSO-11 as V^{5+} has a large quadrupolar coupling constant.

4. Conclusion

V^{4+} species in as-synthesized VAPSO-11 are vanadyl-like and are located in square pyramidal or distorted octahedral structures. The V=O bond distance is short and the π bond is more ionic compared to that in Vanadium-incorporated AFI structures. On calcination, V^{4+} species are converted to V^{5+} species. On reduction, V^{5+} species are converted back to V^{4+} species. In both cases, the vanadium species are shown to be located in square pyramidal or distorted octahedral structures and have a phosphate environment (V–O–P rather than V–O–Si bonds). The reduction of V^{5+} to V^{4+} in VAPSO-11 occurs at a higher temperature due to stronger V–O–P bond compared to V–O–Si of V-silicalite.

Acknowledgements

We are indebted to Dr. P. Ratnasamy and Dr. A.V. Deo for their invaluable discussions. P.S.S. and R.B. thank C.S.I.R. for research fellowships.

References

- [1] N. Tielen, M. Geelen and P.A. Jacobs, *Acta Phys. Chem.*, 31 (1985) 1.
- [2] L. Morosi, L. Stabenow and J. Schwarzmann, FRG Pat. Appl. 2131631, 1981.
- [3] M.S. Rigutto and H. Van Bekkum, *Appl. Catal.*, 68, (1991) L1.
- [4] E.M. Flanigen, B.M. Lok, R.L. Patton and S.T. Wilson, *Eur Pat.* 158,976 (1985).
- [5] C. Montes, M.E. Davis, B. Murray and M. Narayana, *J. Phys. Chem.*, 94 (1990) 6431.
- [6] M.S. Rigutto and H. van Bekkum, *J. Mol. Catal.*, 81 (1993) 77.
- [7] B.M. Lok, C.A. Messina, R.L. Patton, R.T. Gajek, E.M. Flanigen and T.R. Cannan, *US Pat.* 4,440,871 (1984).
- [8] J. Kornatowski, G. Finger, K. Jancke, J. Richter-Mendau, D. Schultze, W. Joswig and W.H. Baur, *J. Chem. Soc., Faraday Trans.*, 90 (14) (1994) 2141.
- [9] A. Ojo and L. McCusker, *Zeolites*, 11 (1991) 460.
- [10] (a) V.R. Choudhary and D.B. Akolekar, *J. Catal.*, 103 (1987) 115. (b) S.G. Hedge, P. Ratnasamy, L.M. Kustov and V.B. Kazansky, *Zeolites*, 8 (1988) 137. (c) J. Das, S.P. Lohokare and D.K. Chakrabarty, *Ind. J. Chem.*, 31 A (1992) 742.
- [11] G. Centi, S. Perathoner, F. Trifiro, A. Aboukais, C.F. Aissi and M.J. Guelton, *J. Phys. Chem.*, 96 (1992) 2617.
- [12] C.J. Ballhausen and H.B. Gray, *Inorg. Chem.*, 1 (1962) 111.
- [13] A.K. Viswanath, *J. Chem. Phys.*, 67 (1977) 3744.
- [14] A. Manoogian and J.A. Mckinnon, *Can. J. Phys.*, 45 (1967) 2769.
- [15] L.J. Boucher, E.C. Tynan and T.F. Yen, *Electron Spin Resonance of Metal Complexes*, Adam Hilger, London, 1969.
- [16] B.I. Whittington and J.R. Anderson, *J. Phys. Chem.*, 95 (1991) 3306.
- [17] D. Kivelson and S.K. Lee, *J. Chem. Phys.*, 41 (1964) 1896.
- [18] V.K. Sharma, A. Wokaun and A. Baiker, *J. Phys. Chem.*, 90 (1986) 2715.
- [19] K. Nowinska and A.B. Wieckowski, *Z. Phys. Chem. NF*, 162 (1989) 231.
- [20] B.R. McGarvey, *J. Phys. Chem.*, 71 (1967) 51.
- [21] M.A. Hitchman, B.W. Moores and R.L. Belford, *Inorg. Chem.*, 8 (1969) 1817.
- [22] G. Brouet, X. Chen, C.W. Lee and L. Kevan., *J. Am. Chem. Soc.*, 114(10) (1992) 3720.
- [23] W.J. Kulinski, S.K. Hoffmann and A.B. Wieckowski, *Phys. Status Solidi (B)*, 96 (1979) 745.
- [24] H. Bosch, B.J. Kip, J.G. van Ommen and P.J. Gellings, *J. Chem. Soc., Faraday Trans.*, 80 (1984) 2479.
- [25] F. Roozeboom, M.C. Mittelmeyer-Hazeleger, J.A. Moulijn, J. Medema, V.J.H. de Beer and P.J. Gellings, *J. Phys. Chem.*, 84 (1980) 2783.
- [26] H. Eckert and I.E. Wachs, *J. Phys. Chem.*, 93 (1989) 6796.
- [27] D. Rehder, *Bull. Magn. Reson.*, 4 (1982) 33.